Karlsruhe Institute of Technology

Sharing is encouraged

EGU23-1292

Continuous seismic monitoring of a geothermal project using Distributed Acoustic Sensing

A case study in the German Molasse Basin

Jerome Azzola[1], Emmanuel Gaucher[1]   [1]Institute of Applied Geosciences, Geothermal Energy and Reservoir Technology

jerome.azzola@kit.edu

Bundesministerium für Wirtschaft und Klimaschutz

INSIDE

Stadtwerke München GmbH
Innovative Energie Pullach
Karlsruher Institut für Technologie

Introduction

We present the results of a **6-month** monitoring period that aimed at testing an integrated system designed to manage the acquisition, the processing and the saving of DAS data collected from behind casing at the **operating Schäftlarnstraße** (SLS) **geothermal project** (Munich, Germany). The data management system links the existing on-site infrastructure to a cloud platform integrated into the company's IT infrastructure. The cloud platform has been designed to deliver both a **secure storage environment** for the DAS records and **optimized computing** resources for their processing.

With a special focus on seismic risk mitigation, we investigate the potential of the monitoring concept to provide sensitive detection capabilities, despite operational conditions, while ensuring efficient data processing, aiming for **real-time monitoring**. Further analysis of the records confirm additional logging capabilities of borehole DAS. We also evaluate the ability of DAS to provide reliable **seismic source description**, in particular in terms of location, moment magnitude, and stress drop. From two detected local seismic events, we demonstrate the relevance of the system for monitoring the SLS-site in an urban environment, while **complementing advantageously the surface seismometer-based monitoring network.**

1 - The Case Study

What - A concept for local seismic monitoring based on DAS, scalable to multiple FOCs / sites, possibly embedded in a Reservoir Management System (RMS).

Where - Schäftlarnstraße geothermal heating plant (Munich) operating the Malm reservoir. Nearest seismometer: SYBAD, borehole 3C at a distance of ~1 km / -180 m uGL.
Fig. 1: focus on TH3 downhole fiber optic cable (FOC).

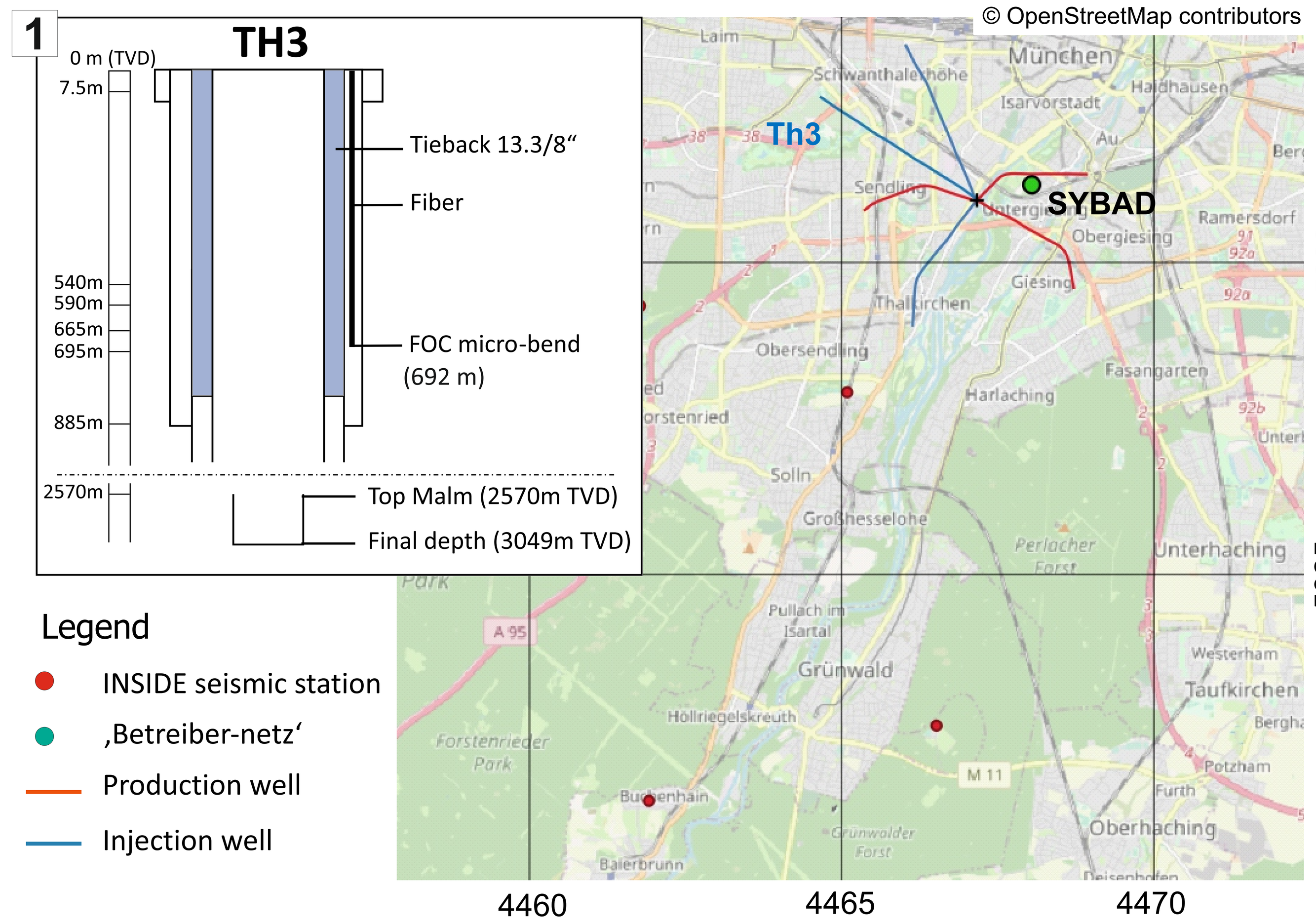

Motivation - borehole DAS, from behind casing, are *a priori* suitable for seismic monitoring in urban context: no well obstruction, smaller distance to monitoring target, noise conditions...

Fig. 2: DAS recordings over the first 100 m during a full week, show the influence of anthropogenic noise at shallow depths.

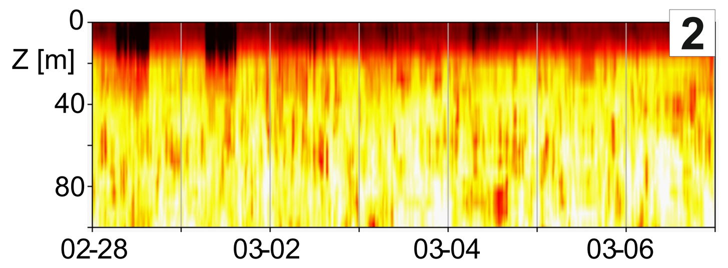

2 - Presentation of the concept for continuous DAS-monitoring

The infrastructure

- Need for scalability / standardization motivated the use of cloud ressources for data storage / processing.
- **Fig. 3**: infrastructure proposed to link the TH3 FOC, the Febus A1-R, the developed IoT cloud platform and the users.

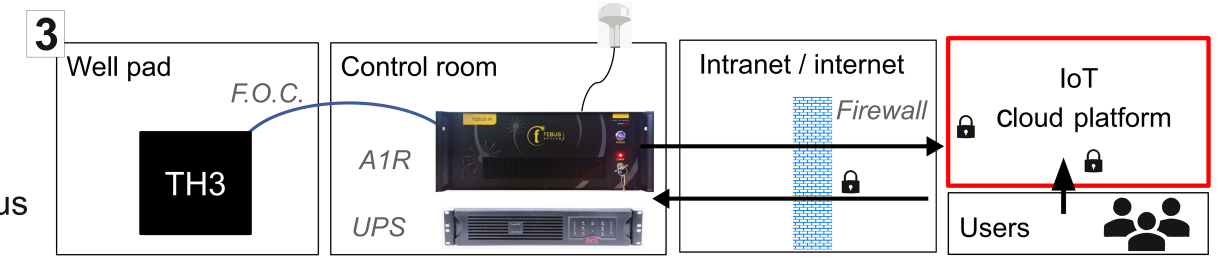

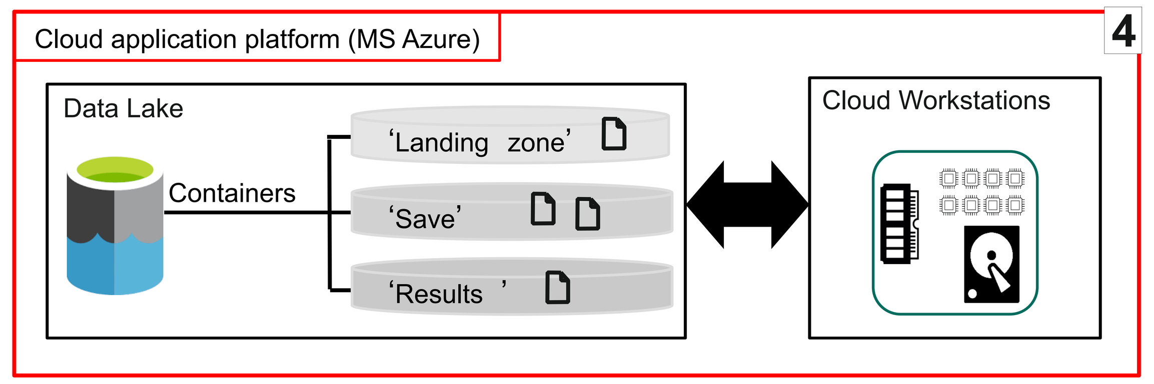

Fig. 4: focus on the cloud platform.

- Based on Microsoft Azure for compatibility with the SWM IT environment.
- For data storage, the Data Lake fulfiles requirements in terms of security, delegation of access rights and connectivity.
- For data processing, cloud workstations provide scalable resources and adapted computing performances.

Data Processing

Fig. 5: flow chart, data recording / processing sequence, separated into

- data /results **archiving** on the Data Lake (center),
- **data triggering** on the cloud workstations for the timely detection of events (left + **Sect. 3**),
- **post-processing** of the detected events for source description (right + **Sect. 4**).

Processing Strain Rate (SR) data blocks allows to control the time delay in actual detection of events (at most, 120% of the block lifetime)

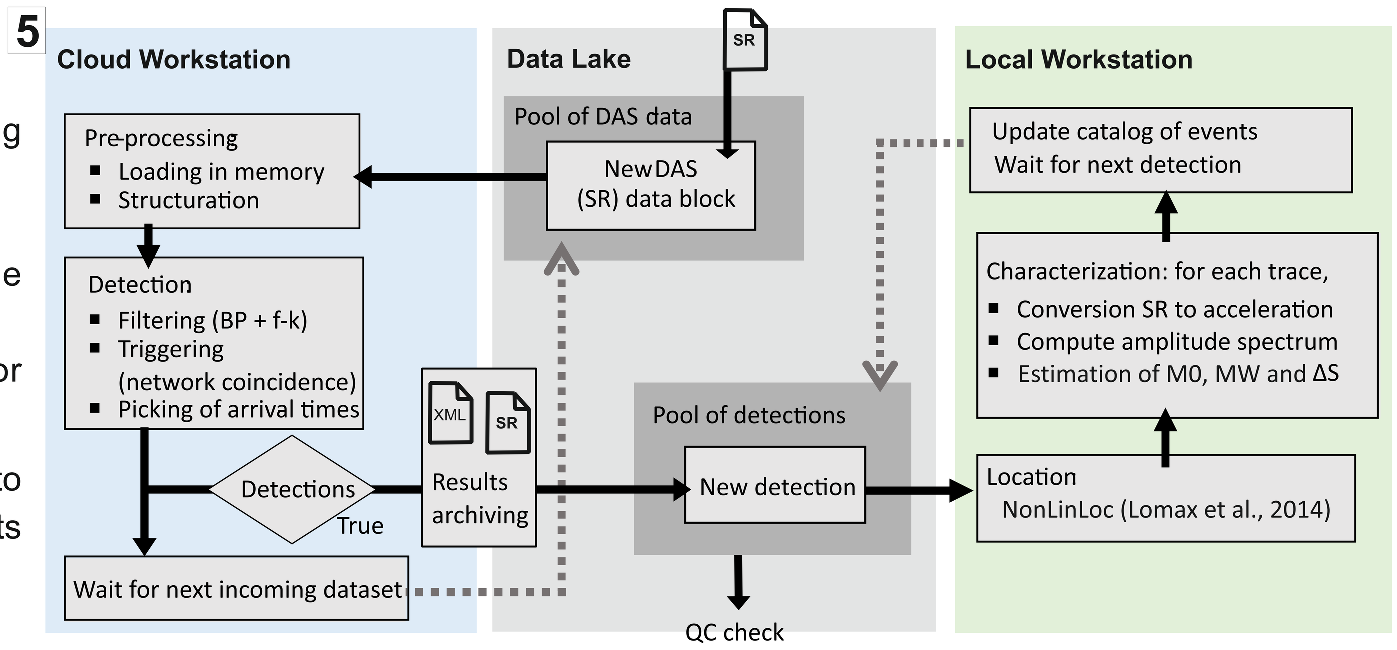

3 - Event Detection on Cloud Workstations

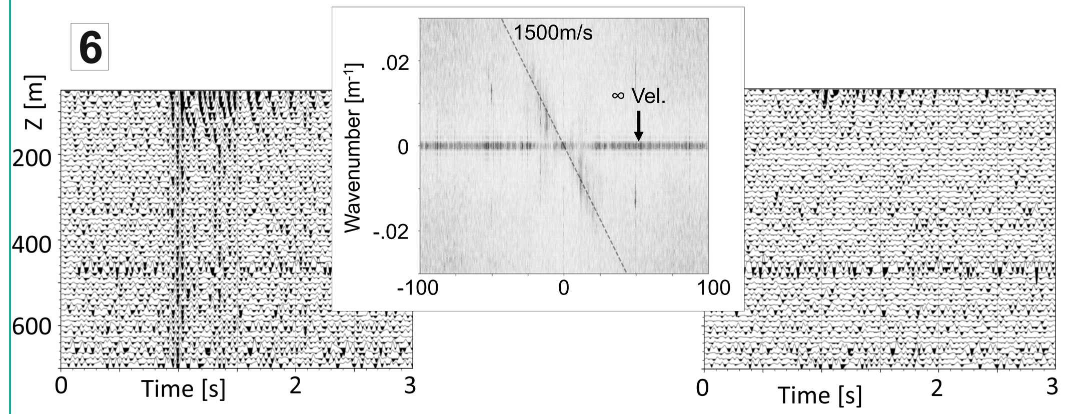

Data Filtering / Denoising

Fig. 6: illustrates the impact of site operations on DAS. Left to right,

- in the t-D domain, shows the coherent propagation of descending signal at ~1500 m/s and instrumental noise around 1 s.
- in the f-k domain, with the line showing the signature of the down-going wave and instrumental noise visible at 0 m^{-1}.
- in the t-D domain, after suppressing energy of known noise sources.

Event Detection

- Automatic event detection: based on a network coincidence trigger and STA / LTA results on all single sensing points.
- Automatic picking (**Fig. 7**): f-k filtering to isolate P (center) or S waves (right panel) with prior access to apparent VP/VS. Individual STA/LTA triggers lead the search for onset time at each sensing point.

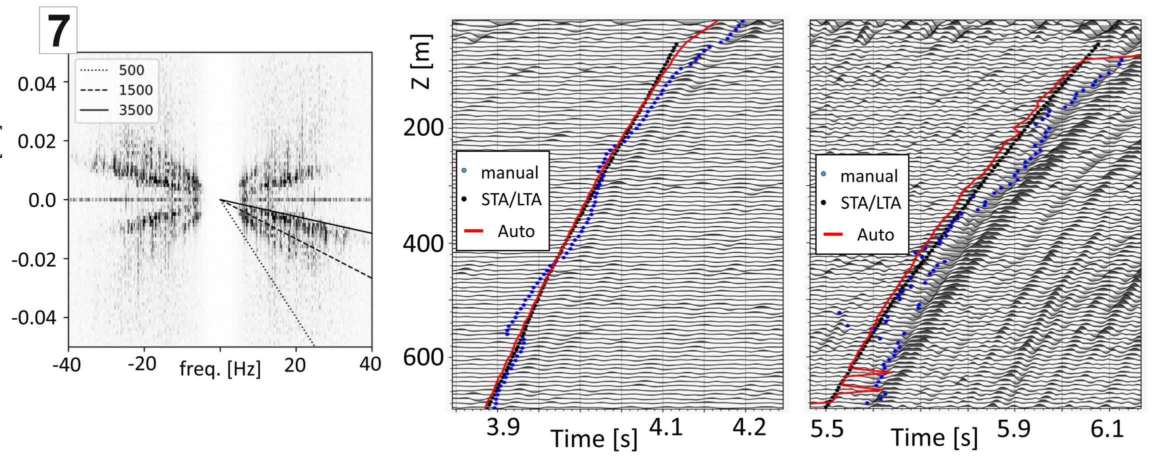

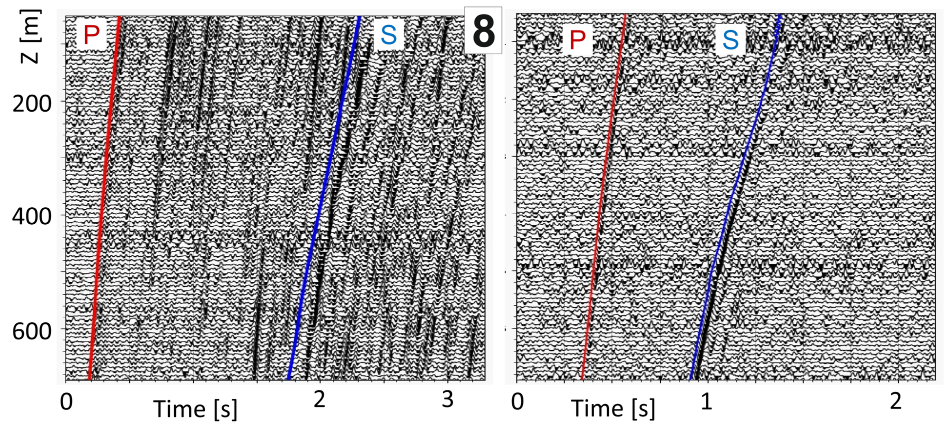

Example of Detections

- Test period (6 months) results in a couple of detections with continuous recording of P/S waves over the optical fiber (**Fig. 8**, with results of the 1st arrival pickings).
- **Left**: February 9, 2022 - local, ML 1.5 seismic event, with an epicenter situated ~10 km from Th3 wellhead. Measured locally in a radius of ~10 km.
- **Right**: April 22, 2022 - **Not** observed by surrounding surface seismometers

4 - Post-Processing of Detections - example of February 09 event

Site characterization

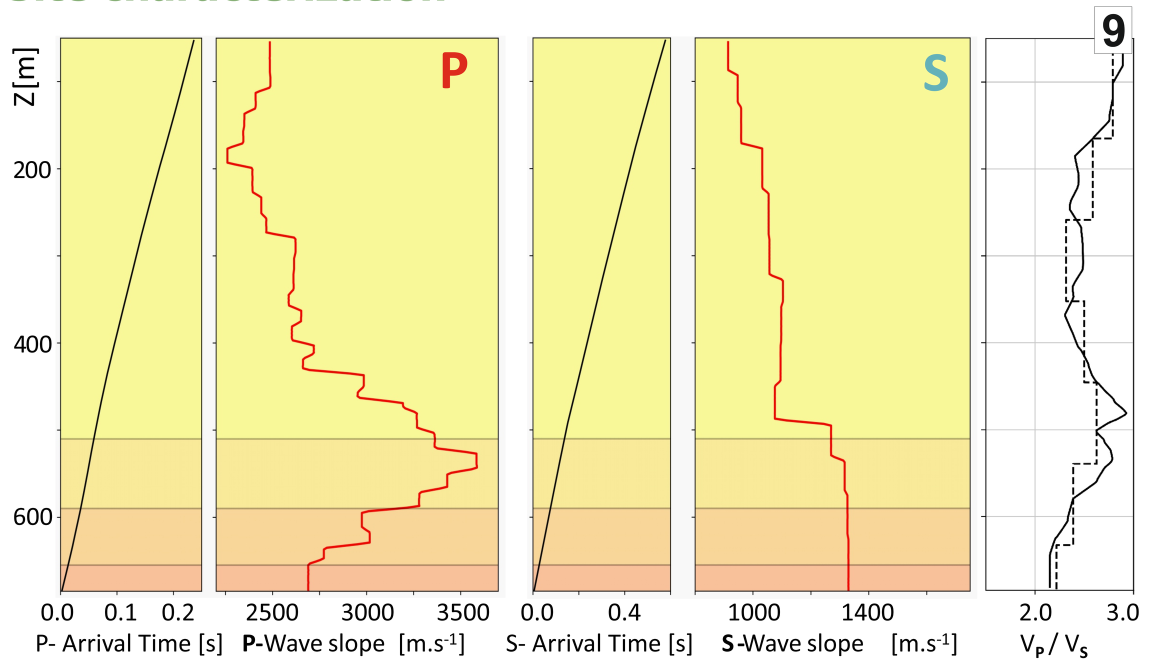

Fig. 9: P- and S-apparent velocities (red) derived from arrival times (black) and used to estimate a VP/VS ratio profile (right). Background colors show lithological units ; the dotted line shows the profile documented by SWM.

Data type conversion

Fig. 10: for a given trace / depth:

- estimation of semblance btw traces in subset of DAS data,
- measurement of slowness as function of time,
- from strain-rate, to acceleration: ACC (t) = SR (t) / slow (t).

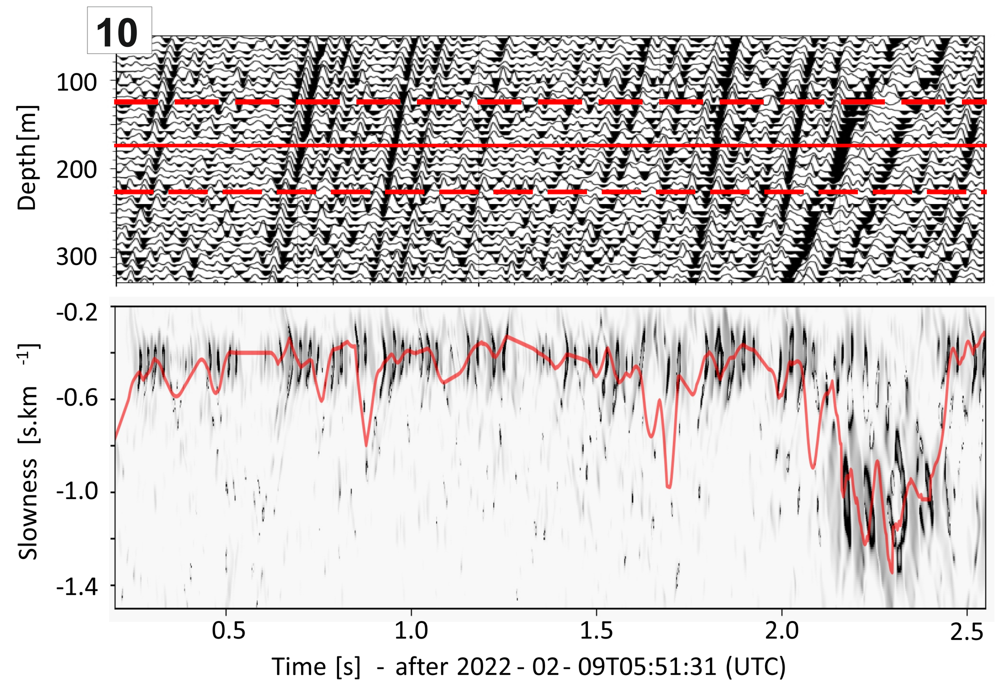

DAS vs seismometer waveform amplitudes

Fig. 11: waveform comparison after data type conversion:

- SYBAD HLZ channel (red) with DAS (black) waveform recorded at depth.
- Goodness-of-fit test (Kristekova et al., 2006) gives „good" fit in phase and comparable amplitudes: SR amplitudes are representative of ground deformation.

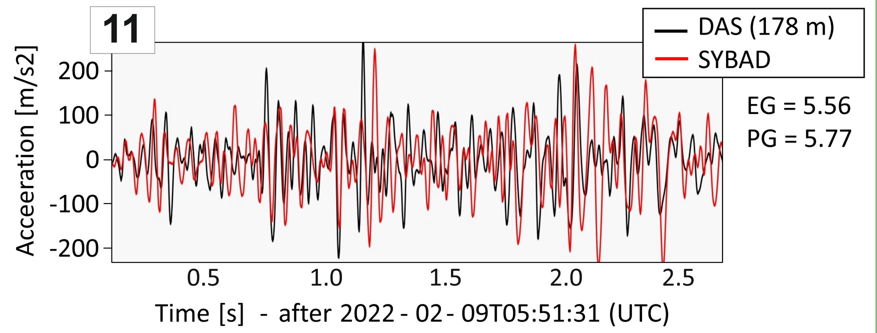

Description of seismic source

Fig. 12: M_0 inversion from single DAS waveform, fitting synthetic and observed amplitude specta ; M_w + ΔS are computed from Madariaga (1976).

$$\ddot{\Omega}(f) = (2\pi f)^2 \left[\Omega_0 / 1 + (f/f_0)^2\right] \exp(-f/f_k)$$

(Anderson & Hough, 1984)

Fig. 13: „ref." M_0 and ΔS values derived from SYBAD seismometer, compared to DAS-estimates (left) and surface network (right). It proves the consistency of DAS measurements.

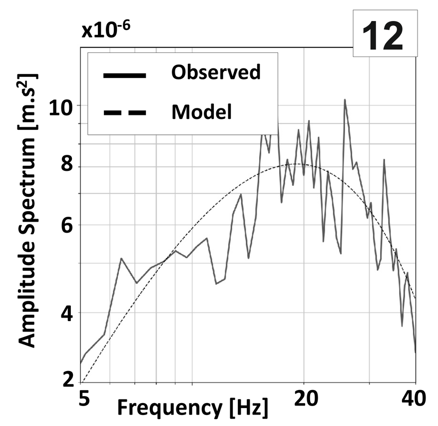

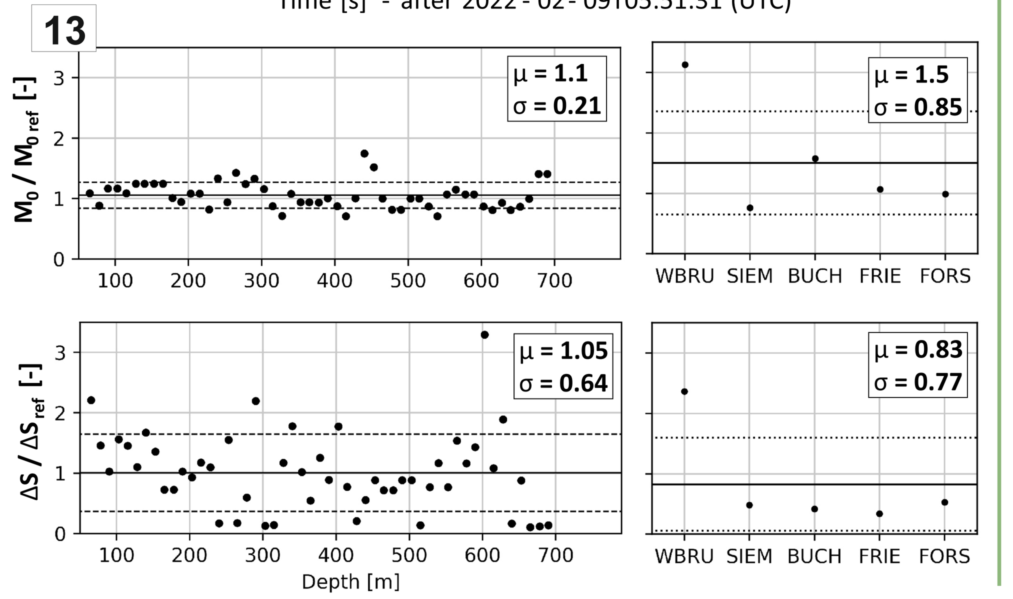

5 - Take Home Messages

- The study consists of a proof of concept, showing the viability of acquiring continuous DAS data in geothermal wells under operational conditions, while efficiently managing and processing the large and continuous flow of DAS records using cloud-based resources.
- The detection sensitivity of the system, which is higher than that of surrounding 3C seismometers, shows that DAS along a cemented fiber behind the casing is suitable for geothermal site (micro-) seismic monitoring, despite the context (flowing well, urban environment).
- The post-processing results show that the DAS amplitudes can be used in a quantitative approach to provide a reliable description of the seismic source, provided that the source is located.
- The flexibility of the infrastructure, in terms of storage capacity and processing resources, opens up prospects for near-real-time data processing and extension to additional monitoring components.
- The system could be the backbone of a reservoir management system aimed at driving the geothermal reservoir operations to mitigate induced seismic risk.

Acknowledgments

This work was conducted in the frame of the INSIDE project, supported by the German Federal Ministry for Economic Affairs and Climate Action and the Project Management Jülich (PtJ). The authors thank the project partners IEP, SWM and Erdwerk for their cooperation.

References

Lior, I. et al..: Strain to ground motion conversion of distributed acoustic sensing data for earthquake magnitude and stress drop determination, 10.5194/se-12-1421-2021, 2021.

Anderson, J. G. and Hough, S. E.: A model for the shape of the fourier amplitude spectrum of acceleration at high frequencies, 10.1785/BSSA0740051969, 1984.

Kristeková, M., et al.: Time-frequency goodness-of-fit criteria for quantitative comparison of time signals, 2009.

Madariaga, R.: Dynamics of an expanding circular fault, 10.1785/BSSA0660030639, 1976.

Lomax, A., et al.: Earthquake Location, Direct, Global-Search Methods, 10.1007/978-3-642-27737-5_150-2, 2014.